

ANALYSIS OF THE HEAVILY BEAM-LOADED SOLEIL RF SYSTEM

A. Mosnier, F. Orsini, SOLEIL, Gif/Yvette (France)
 B. Phung, CEA/DAPNIA, Saclay (France)

Abstract

The RF system of the SOLEIL light source involves superconducting cavities and is working in the heavily beam-loaded limit. Fast amplitude and phase feedback loops provide the required stability of the rf system with particle beam. The steady-state behaviour is analysed using conventional feedback theory, whereas transient beam-loading, arising for example from beam injection or some gap in the bunch train is studied with the help of a numerical code simulating the beam-cavity interaction and feedback loops.

1 INTRODUCTION

The RF system of the SOLEIL Storage Ring has to compensate the energy lost by synchrotron radiation and to provide the RF voltage for a proper longitudinal focalisation. Two single cells superconducting cavity are driven by one klystron, transferring 200 kW per cell to the beam for the nominal beam current of 500 mA. The parameters of the RF system are given in Table 1.

Table 1: RF system parameters

Frequency (MHz)	352.2
Harmonic number	396
Energy loss / turn (keV)	800
Total RF voltage (MV)	4
Total beam power (kW)	400
Geometric impedance (Ω)	45
Loaded Q	$2 \cdot 10^5$
Beam-loading parameter Y	5
Tuning angle Ψ (degree)	-78.5

With compensation of reactive beam-loading, and operating at the optimal coupling ($\beta \gg 1$), the SC cavity-beam system would be, without any feedback, just at the limit of the Robinson stability [1]. Fig.1 shows the unstable region (gray) in the Y - ψ diagram.

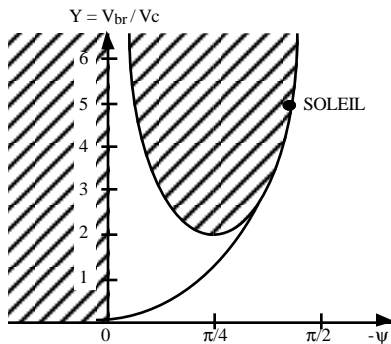


Fig. 1 : SOLEIL stability diagram

2 FREQUENCY ANALYSIS

With the aim of studying the stability of the RF system, with and without feedback, by means of the conventional feedback theory, we recall below the transfer functions (with the Laplace operator p), as defined in [2], but with somewhat different notations :

- Cavity-to-beam transfer function (n=0 dipole mode)

$$\delta\phi_b = F_{\phi a} \delta v_c + F_{\phi\phi} \delta\phi_c$$

$$F_{\phi a} = -\frac{1}{\tan \phi_s} \frac{\omega_s^2}{p^2 + \omega_s^2} \quad F_{\phi\phi} = \frac{\omega_s^2}{p^2 + \omega_s^2}$$

- Beam-to-cavity transfer function

$$\begin{pmatrix} \delta v_c \\ \delta\phi_c \end{pmatrix} = \begin{pmatrix} G_{aa} & G_{a\phi} \\ G_{\phi a} & G_{\phi\phi} \end{pmatrix} \begin{pmatrix} \delta v_b \\ \delta\phi_b \end{pmatrix} \quad \text{with} \quad \begin{matrix} G_{aa} = G_{\phi\phi} \\ G_{a\phi} = -G_{\phi a} \end{matrix}$$

$$G_{aa}(p) = G_1(p) \cos \phi_s + G_2(p) \sin \phi_s$$

$$G_{\phi a}(p) = -G_1(p) \sin \phi_s + G_2(p) \cos \phi_s$$

The functions G_1 and G_2 are given below for 3 cases :

1. without any feedback

$$G_1(p) = -Y \frac{1 + \tau p}{(1 + \tau p)^2 + \tan^2 \psi}$$

$$G_2(p) = -Y \frac{\tan \psi}{(1 + \tau p)^2 + \tan^2 \psi}$$

2. with direct RF feedback [3] of loop gain G

$$G_1(p) = -Y \frac{1 + G + \tau p}{(1 + G + \tau p)^2 + \tan^2 \psi}$$

$$G_2(p) = -Y \frac{\tan \psi}{(1 + G + \tau p)^2 + \tan^2 \psi}$$

3. with fast Amplitude and Phase feedback

(assuming equal loop gains $G_I = G_Q = G$)

$$G_1(p) = -Y \frac{1 + G(1 + Y \cos \phi_s) + \tau p}{D(p)}$$

$$G_2(p) = -Y \frac{\tan \psi + G(\tan \psi + Y \sin \phi_s)}{D(p)}$$

where the denominator $D(p)$ is

$$\left[1 + G(1 + Y \cos \phi_s) + \tau p\right]^2 + \left[\tan \psi + G(\tan \psi + Y \sin \phi_s)\right]^2$$

The schematic circuit of this last case is drawn on Fig. 2. The drive current is modulated by in-phase and in-quadrature signals, proportional to amplitude and phase errors, through an I/Q modulator. The generator current can be written as

$$\tilde{I}_g = \tilde{I}_{go} \cdot \left[1 + G_I (V_{set} - V_c) / V_c + j G_Q (\phi_{set} - \phi_c) \right]$$

where G_I and G_Q are the amplitude and phase loop gains.

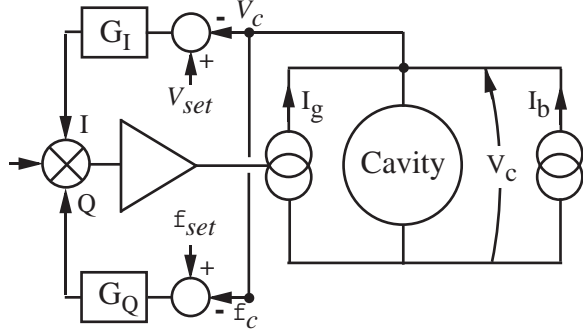


Fig. 2 : Schematic of the fast amplitude and phase feedback loops

The resulting beam-loading parameter Y limits, deduced from Nyquist or Routh criteria, are given below with reactive beam loading compensation ($\tan \psi = -Y \sin \phi_s$)

With **direct RF feedback**, the high-intensity Robinson limit is increased by the factor $(1+G)$

$$\Rightarrow Y < \frac{1+G}{\cos \phi_s}$$

With **amplitude and phase feedback**, the dynamic behaviour is similar to the direct RF feedback (assuming identical I and Q loop G gains), but with an effective loop gain $G \rightarrow G(1+Y \cos \phi_s)$, which increases automatically with the beam current; the system is then always stable, as soon as the gains are larger than 1. Since a fast phase feedback is anyway needed for SOLEIL, because of the high level of time stability required by light lines users, the amplitude and phase feedback system was chosen.

The damping rates of the cavity-beam system were calculated for the SOLEIL ring parameters. They are given by the real part of the poles of the closed-loop transfer function, i.e. the roots of a 4th order characteristic equation. Fig. 3 shows the evolution of the damping rates as function of the gain of the amplitude and phase loops. It is worthwhile noting that the highest damping rate is achieved for a very modest gain ($G=2$). For higher gains, the cavity voltage (amplitude and phase) is nearly constant and the longitudinal beam dynamics are then decoupled. Only the synchrotron radiation will be effective to damp beam oscillations.

Furthermore, since the Q of SC cavities is relatively high, the gain limitation due to a time delay of the loops is not severe : the system is stable even with an effective loop gain of 100, assuming an overall time delay of 1.5 ms, a very pessimistic value.

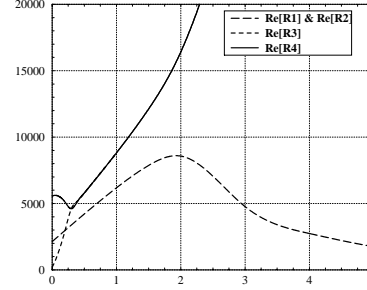


Fig. 3 : Damping rates of the cavity-beam system (SOLEIL parameters)

3 RESULTS OF SIMULATIONS

In order to study the dynamic behaviour of the RF system, under various perturbations, a numerical code was written, simulating the beam-cavity interaction and the feedback loops. The sequence is the following : energy and phase of the bunches are changed at each turn, according to the classical synchrotron dynamics; at each traversal of a bunch through the cavities, the voltage is modified by the induced wake; between two successive passages, the evolution of the cavity voltage is calculated by Runge-Kutta integration of the cavity differential equations. For example, in case of amplitude and phase feedback, this differential equation can be written

$$\tau (\dot{V}_c + i V_c \dot{\phi}_c) + (1 - i \tan \psi) V_c = R I_{go} e^{i(\phi_{go} - \phi_c)} \times \left[1 + G_I (V_{set} - V_c) / V_{set} + i G_Q (\phi_{set} - \phi_c) \right]$$

We first checked the previous results, predicted by the feedback theory, without any additional perturbation. On Fig. 4, we can see that the beam cannot kept stable without feedback (left), whereas the amplitude and phase feedback is able to stabilize the beam at any current when the gain of the amplitude and phase loops is larger than unity. On these examples, The beam was launched with an initial phase error of 10° .

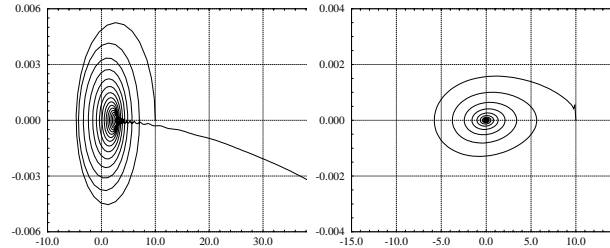


Fig. 4 : Bunch motion in the longitudinal phase space ($\Delta E/E - \Delta \phi$) w/o feedback (left) and with feedback (right)

4 EXTERNAL PERTURBATIONS

The effect of an eventual **beam gap**, to cope if necessary with the ion-trapping problem, was estimated.

We would like to restrict the bunch phase modulation, induced by the gap, to about 1/10 degree, in such a way that the time jitter, as seen by the experiments is around 1 ps. In steady-state, the phase of each bunch of the train is fixed by radiation damping and the phase modulation is determined by the size of the beam gap. Since SC cavities have a low R/Q and high accelerating voltage, the phase modulation is approximately linear (Fig. 7). The feedback system, whose effect is to zeroing the average bunch phase, and radiation damping are both in operation in this simulation. The maximum bunch gap allowed is 15%, giving a bunch phase modulation of about $\pm 0.12^\circ$ and a cavity voltage modulation of about $\pm 0,05\%$.

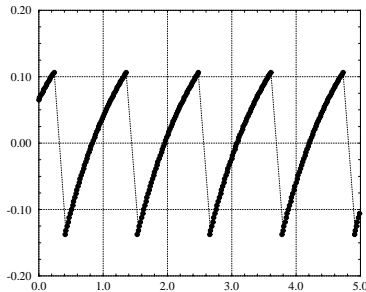


Fig. 5 : Beam phase fluctuation due to a 15 % beam gap (feedback 'ON').

Microphonics noise is the most harmful effect for SC cavities, because of the narrow bandwidth and poor stiffness of the mechanical structure. Although a single klystron is feeding a pair of cavities, we are confident that no ponderomotive instabilities will occur with feedback, because the Q of the cavity is fairly low (of the order of $2 \cdot 10^5$). However, mechanical modes can be excited by external perturbations, like the cryogenics system for example. Simulations were performed with different mechanical resonance frequencies and different modulation amplitudes. Fig. 6 shows for example the energy and phase fluctuations of the beam with a mechanical oscillation at 1 kHz and generating a cavity phase modulation of $\pm 20^\circ$. After performing somewhat chaotic transient phase and energy oscillations, the beam reaches a stable trajectory (thick line) with a phase magnitude of the order of $\pm 0.1^\circ$, with closed feedback loops (gain 40 dB).

As soon as one single klystron feeds multiple cavities, the **calibration in phase and in amplitude** for the vector sum reconstruction, which is the sole quantity we can control, becomes a crucial point. Any time-varying perturbation, like microphonics, will induce a fluctuation of the actual total voltage, even if we assume a perfect feedback system. Fig. 7 shows the rms phase fluctuation as a function of the phase calibration error (an amplitude calibration error of 10% was assumed), for tuning angle variations between -10° and $+10^\circ$, due to microphonics. This effect is significant (two cavities only are involved) and final phase will be carefully adjusted with beam.

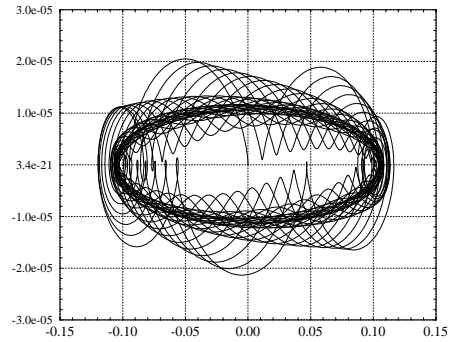


Fig. 6 : Bunch energy and phase oscillations, excited by a mechanical mode (feedback 'ON').

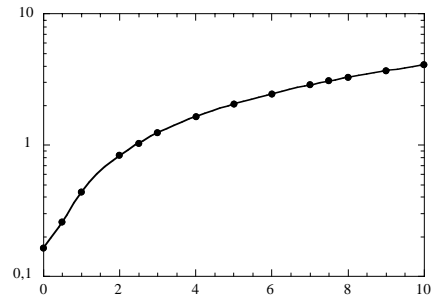


Fig. 7 : rms phase fluctuation vs phase calibration error (degrees).

5 CONCLUSION

An analog control module (Fig. 8), using I/Q modulators for fast amplitude and phase feedback loops is in progress. We are looking at eventual digital loops, using fast DSPs, which could offer further flexibility.

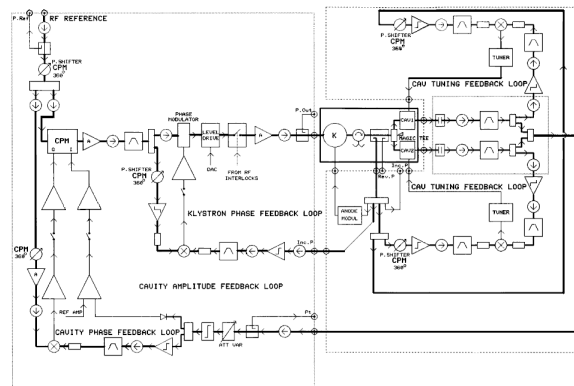


Fig. 8 : Drawing of the analog control module.

REFERENCES

- [1] K.W. Robinson, "Stability of beams in radiofrequency systems", CEAL-1010, Feb. 1964.
- [2] F. Pedersen, "Beam Loading Effects in the CERN PS Booster", IEEE Trans. Nucl. Sci. NS-32, 1985.
- [3] D. Boussard, "Control of Cavities with High Beam Loading", IEEE Trans. Nucl. Sci. NS-32, 1985.